frontiers | Frontiers in Electronic Materials

REVIEW
published: 24 May 2022
doi: 10.3389/femat.2022.913280

Tetrahedrite Thermoelectrics: From Fundamental Science to Facile Synthesis

Daniel P. Weller[1] *and Donald T. Morelli*[2]*

[1]School of Mathematical and Physical Sciences, University of New England, Biddeford, ME, United States, [2]Department of Chemical Engineering & Materials Science, Michigan State University, East Lansing, MI, United States

Thermoelectric materials have a long and storied history in the research and development of semiconductor materials, being the first such class of materials to be investigated. Thermoelectrics may be used to convert heat to electricity or, alternatively, to liberate or absorb heat upon electrical excitation. They thus find application in thermoelectric generators for converting heat from a primary source or a waste stream to useful electrical power, and as solid state heating and cooling devices. In spite of their great potential in such important applications, thermoelectrics have suffered from a number of drawbacks that have hindered their utilization on a large scale. Chief among these is the fact that most high performance thermoelectric materials are comprised of elements that are in relatively low abundance. Additionally, their synthesis typically involves complex and multi-step processes, hindering manufacturability. Thermoelectric materials derived from Earth-abundant sources are thus of strong current interest, from both scientific and economic points of view. One of these, the family of semiconductors based on tetrahedrite compounds, has generated enormous interest over the last decade due to not only its potential low cost, but also for its fascinating science. In this review, we summarize the state of the art of tetrahedrite as a thermoelectric, with special emphasis on the relationship between crystal structure and bonding in the crystal and its unusually low lattice thermal conductivity; on its fascinating electronic structure; and on the wide array of compositions that have been synthesized and whose thermoelectric properties have been studied. We further highlight some rapid and facile synthesis techniques that have been developed for these compounds which, in combination with their potential low material cost, may open the door to widespread application of these fascinating materials.

Keywords: crystal structure, electronic structure, thermoelectric, thermal conductivity, facile synthesis

OPEN ACCESS

Edited by:
Ctirad Uher,
University of Michigan, United States

Reviewed by:
Wei-Di Liu,
University of Southern Queensland, Australia
Yun Zheng,
Jianghan University, China

***Correspondence:**
Donald T. Morelli
dmorelli@egr.msu.edu

Specialty section:
This article was submitted to Thermoelectric Materials, a section of the journal Frontiers in Electronic Materials

Received: *05 April 2022*
Accepted: *03 May 2022*
Published: *24 May 2022*

Citation:
Weller DP and Morelli DT (2022) Tetrahedrite Thermoelectrics: From Fundamental Science to Facile Synthesis. Front. Electron. Mater. 2:913280. doi: 10.3389/femat.2022.913280

1 INTRODUCTION: THE CONUNDRUMS OF THERMOELECTRICITY

Thermoelectricity encompasses the collective effects that involve the conversion of a temperature difference to electricity and vice versa. These effects may be implemented to generate electrical power from primary or waste sources of heat, or inversely to provide all-solid-state heat pumping (i.e., climate control) under electrical activation (Goldsmid, 1960). However, in contrast to other energy conversion technologies such as photovoltaics, thermoelectrics have not enjoyed large-scale application in power generation due to a combination of several factors, including low conversion efficiency, high cost, and complex manufacturing methods. In spite of this (or perhaps, depending on

one's point of view, because of it), work on new thermoelectric materials and methods of manufacture continues today. Researchers hope that low cost materials and facile synthesis techniques will unlock the enormous potential this technology has for recovering the gargantuan amount of energy—nearly two thirds of that generated—that is lost in the form of waste heat in industrial, commercial, and residential energy production in the US economy (US Department of Energy and Lawrence Livermore National Laboratory, 2016)

The ability of a thermoelectric (TE) material to function effectively in such applications is determined by a combination of its thermal and electronic transport properties, and is succinctly captured in the thermoelectric figure of merit:

$$z = \frac{S^2\sigma}{k} \tag{1}$$

where S is the Seebeck coefficient (i.e., thermoelectric power), σ is the electrical conductivity, and k is the total thermal conductivity of the material in question. As the dimensions of this quantity z are inverse temperature, one frequently defines a dimensionless quantity, zT, the product of z and the absolute temperature T:

$$zT = \frac{S^2\sigma}{k}T \tag{2}$$

It is self-evident that for a TE material to have so-called "high zT," it should possess a combination of large Seebeck coefficient, high electrical conductivity, and low thermal conductivity. Further, noting that the electrical conductivity may be expressed in terms of the charge carrier concentration n and the charge carrier mobility μ as $\sigma = ne\mu$, and that the thermal conductivity is composed of electronic (k_E) and lattice (k_L) components, the dimensionless figure of merit may be expressed as:

$$zT = \frac{S^2ne\mu}{k_E + k_L}T \tag{3}$$

An examination of **Equation 3** reveals two fundamental conundrums of thermoelectricity. Firstly, while the conductivity increases with increasing charge carrier concentration, the Seebeck coefficient has the opposite trend; while insulators can have very large Seebeck coefficient, S in metals is usually very small. One cannot simply increase σ to increase zT. Secondly, since the electronic part of thermal conductivity is governed by the Wiedemann-Franz law, and thus is coupled to the electrical conductivity, again increasing σ has diminishing returns as k_E will also become large. The solution of these conundrums leads one naturally to focus on moderately to heavily doped semiconductors in which both the Seebeck coefficient and conductivity can be substantial, and yet the latter is not so large as to yield large k_E (**Figure 1**). Finally, then returning to **Eq. 3**, one must also seek materials in which the lattice thermal conductivity k_L is also small in order to ultimately achieve high zT.

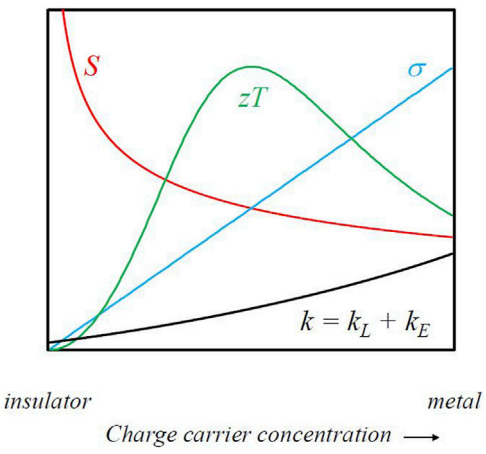

FIGURE 1 | The conundrums of thermoelectricity. While electrical conductivity σ increases with increasing charge carrier concentration, Seebeck coefficient S shows the opposite trend. Additionally, electronic thermal conductivity k_E increases with increasing σ. Finally, lattice thermal conductivity k_L must remain low. All of these factors must be balanced to achieve high zT.

By the middle of the 20th century, the main factors determining the lattice thermal conductivity of crystalline solids were well understood (Akhiezer, 1940; Leibfried and Schlömann, 1954; Lawson, 1957; Julian, 1963), and it was realized that the best candidate materials for low lattice thermal conductivity would comprise atoms of heavy atomic mass and would possess complex crystal structures with low Debye temperatures. Indeed, the first successful thermoelectrics, PbTe (Ioffe, 1957) and Bi_2Te_3 (Goldsmid and Douglas, 1954), which possess zT values near 0.5, were developed using these guiding principles. Shortly thereafter, based on numerous studies of point defect scattering of phonons (Geballe and Hull, 1955; Callaway and von Baeyer, 1960; Klemens, 1960; Abeles, 1963), further improvements were realized by employing alloy scattering to reduce k_L. Other notable advances in thermoelectric material design and discovery included the concept of phonon glass-electron crystal introduced by Slack (Slack and Rowe, 1995), which led to the successful development of skutterudite (Slack and Rowe, 1995) and clathrate (Nolas et al., 2002) based thermoelectric materials systems, and that of nanostructuring (Dresselhaus et al., 2007), which has been used successfully to design many materials systems, some with thermoelectric figure of merit in excess of two.

While these advances in thermoelectric materials have been notable, their use in large scale applications for waste heat recovery or thermoelectric power generation has been greatly hampered due to several factors. First, most high performance TE materials contain low abundance elements, which are costly to incorporate into large-scale manufacturing. This is not a coincidence because the "traditional" approaches to lowering thermal conductivity require heavy mass elements, which are in low abundance in the Earth's crust. Second, many high-performance materials, a good example being the "hierarchical" structures based on PbTe (Biswas et al., 2012),

rely on the careful construction of a defect and impurity profile which can be difficult to maintain in a large-scale production scenario. Third, the standard methods of synthesizing thermoelectric materials, for instance, vacuum melting and recrystallization, are not amenable to production of large-surface area structures that would be most suitable for taking advantage of heat sources. Thus, the need for earth-abundant TE materials that can be synthesized with facile methods that are easily scalable is quite urgent.

2 OVERVIEW OF TETRAHEDRITE THERMOELECTRICS

To best understand the historical development of tetrahedrite thermoelectrics and some of their structural properties, it is useful to put them into context with other copper-containing semiconductors. This is a large and important family of materials. Several of them can be thought of as higher order derivatives of traditional diamond-structure II-VI semiconductors such as ZnSe (Goryunova, 1965). To see why this is so, first imagine that one takes the zincblende structure of ZnSe, and simply "doubles" the unit cell (i.e., stacks one zincblende unit cell on top of another), creating a Zn_2Se_2 structure. With two Zn atoms possessing two valence electrons each, and two Se atoms possessing six valence electrons each, there are a total of 16 electrons available for sharing among the bonds of these four atoms, or an average of four electrons per atom that is characteristic of the "diamond-like" family of materials. Now, one simply replaces the two Zn^{2+} ions with one monovalent Cu^{1+} and one trivalent Ga^{3+} ion, thus creating the compound $CuGaSe_2$. Once again counting electrons [1 + 3 + (2 × 6) = 16], an average electron count of four per atom is maintained. In this way one can produce several different Cu-based "chalcopyrite" diamond-like semiconductors of the form Cu-III-VI_2 using other combinations of group II and group VI atoms. Going a step further, "tripling" the ZnSe unit cell (Zn_3Se_3), and replacing two divalent zinc ions with two monovalent Cu ions, and the remaining divalent Zn ion with a tetravalent ion such as Sn, one can create compounds of the type Cu_2SnSe_3 which again maintain an average of four electrons per atom [(2 × 1) + 4 + (3 × 6) = 24 electrons, spread across six atoms]. Finally, in a similar fashion, by "quadrupling" the ZnSe unit cell (Zn_4Se_4) and replacing the four divalent Zn^{2+} ions with three monovalent Cu^{1+} ions and a pentavalent Sb^{5+} ion, one creates the diamond-like semiconductor Cu_3SbSe_4, again with an average of four electrons per atom [(3 × 1) +5 + (4 × 6) = 32 electrons, spread across eight atoms]. Several ternary copper-containing compounds constructed in this fashion, including $Cu_3SbSe_{4-x}S_x$ solid solutions (Skoug et al., 2011), Cu_2SnSe_3 (Skoug et al., 2010), $CuInTe_2$ (Liu et al., 2012), $CuGaTe_2$ (Plirdpring et al., 2012), and Cu_5FeS_4 (Qiu et al., 2014) have been shown to possess dimensionless figure of merit close to or even exceeding unity.

Although close in composition to some of the compounds described above, tetrahedrite (base composition $Cu_{12}Sb_4S_{13}$) possesses a crystal structure considerably more complex than that of its close relative Cu_3SbS_4, and this complex crystal structure is key for understanding the very low lattice thermal conductivity of these compounds. Interestingly, tetrahedrites are naturally-occurring minerals, and in fact are one of the most prevalent sulfosalts on Earth. Natural tetrahedrites are typically of the general chemical composition $Cu_{12-x}Tr_x(Sb,As)_4S_{13}$ where Tr can be one or more of several transition metal elements, including Cu, Zn, Mn, and Ni (Makovicky and Moller, 1994). Tetrahedrite with As on the Sb site is known as tennantite, and the tetrahedrite-tennantite pair forms a complete solid solution. As we shall see, a variety of different tetrahedrite compositions have been synthesized in the laboratory. The structure has shown to be capable of incorporating various atoms on different sites. For example, in additional to the transition metal and As substitutions mentioned above, tetrahedrites have also been synthesized with Bi and Te on the Sb site, and Se on the S site.

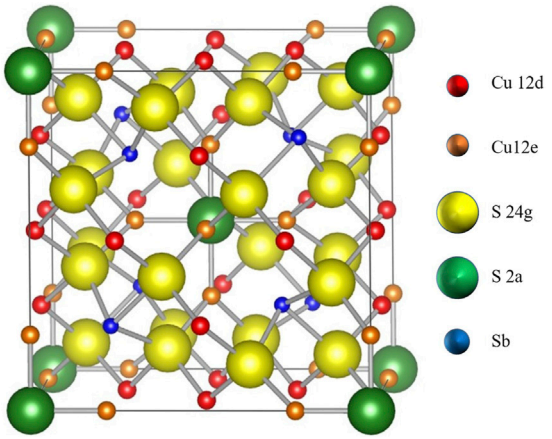

FIGURE 2 | The $Cu_{12}Sb_4S_{13}$ unit cell. There are two crystallographically distinct copper sites, Cu 12 d (red atoms) and Cu 12e (orange atoms). There are also two distinct sulfur sites, S 24 g (yellow atoms) and S 2a (green atoms). There is one distinct antimony site (blue atoms).

3 CRYSTAL STRUCTURE AND BONDING

The outstanding feature of tetrahedrite thermoelectrics is the extremely low intrinsic thermal conductivity. Several studies have focused on understanding the origin of this behavior, and how it arises from several features of the bonding and crystal structure in these compounds.

Because of their prevalence in the Earth's crust and their importance as copper ores, tetrahedrites have a long history of study in the field of geology. The $Cu_{12}Sb_4S_{13}$ unit cell, shown in **Figure 2**, is a body-centered cubic system with $I\bar{4}3m$ symmetry (Wuensch, 1964) and contains 58 atoms per unit cell. Unlike the Cu-based diamond-like semiconductors described above, which exhibit predominantly tetrahedral bonding, the tetrahedrite structure is comprised of several different atomic coordinations and bonding types. These are best understood by considering various structural sub-groups which comprise the overall cubic structure, as depicted in **Figure 3** (Pfitzner et al.,

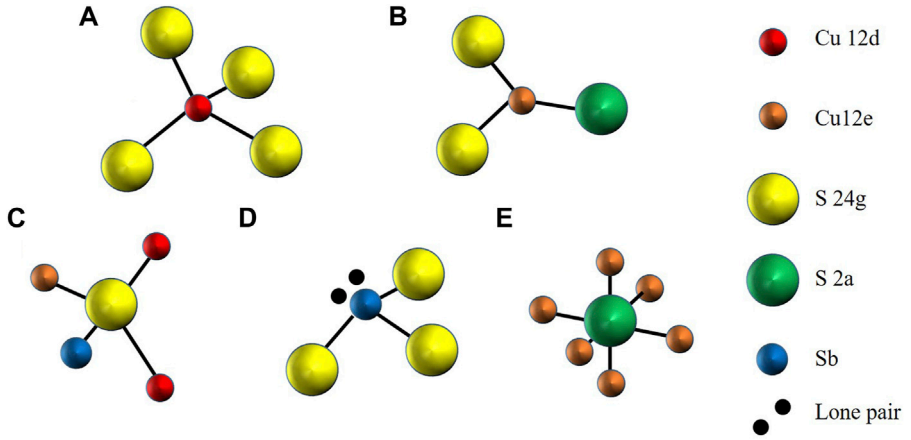

FIGURE 3 | Structural sub-units in tetrahedrite: **(A)** red tetrahedrally coordinated Cu12d; **(B)** orange trigonally coordinated Cu12e; **(C)** yellow tetrahedrally coordinated S24g; **(D)** blue trigonally coordinated Sb, with protruding lone pair electrons (black); and **(E)** green octahedrally coordinated S2a.

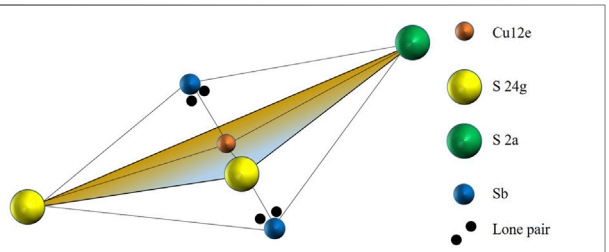

FIGURE 4 | The Sb-CuS_3-Sb bipyramid in tetrahedrite. The Cu12e site (orange) is trigonally coordinated by two S24g atoms (yellow) and one S2a atom (green). Two Sb atoms (blue) reside above and below the trigonal plane. Each Sb atom possesses a set of lone-pair electrons (black) that protrude toward the Cu12e.

1997). Within this structure there are two unique Cu sites (12d and 12e), one Sb site (8c), and two S sites (24g and 2a) (Lai et al., 2015). Each Cu12d atom (**Figure 3A**) is tetrahedrally coordinated by four S24g atoms, whereas each Cu12e atom (**Figure 3B**) is trigonally coordinated to two S24g atoms and one S2a atom. Every S24g (**Figure 3C**) is tetrahedrally coordinated to two Cu12d atoms, one Cu12e atom, and one Sb atom. On the other hand, each Sb atom (**Figure 3D**) is coordinated by three S24g atoms and a protruding lone pair, such that the Sb lone pair creates a void-like pocket in the structure. Lastly, each S2a atom (**Figure 3E**) is in an octahedral coordination with six Cu12e atoms. Therefore, the crystal structure of tetrahedrite is quite intricate and displays an array of distinct atomic bonding coordinations, and, as we shall see shortly, these have important implications in the context of low lattice thermal conductivity of tetrahedrite. We first note that, unlike the derivative ternary diamond-like semiconductors such as Cu_3SbSe_4 discussed above for which Sb is in a tetrahedral coordination and possesses a nominal valence of Sb^{5+}, in the tetrahedrite structure Sb is in trigonal coordination and nominally in the trivalent Sb^{3+} state. This gives rise to two antimony electrons in a non-bonding state, forming the aforementioned lone pair. In the trigonal coordination, the Cu12e atom is sandwiched between two Sb atoms such that the Sb lone pairs are oriented towards the Cu12e atom; this bonding effectively yields a trigonal bipyramidal arrangement for the Cu12e atom with two Sb lone pairs on the axial sites (**Figure 4**). Further, as shown in **Figure 4**, these lone-pair-endowed Sb atoms lie both above and below the trigonal plane formed by Cu(2) and three S atoms. One can thus view this entire molecular sub-unit as a Sb [CuS_3]Sb trigonal bipyramid. In such a scenario, this bipyramidal sub-unit bears a striking resemblance to "cage-like" structural units in poor thermal conductors such as skutterudite and clathrate compounds.

Each $Cu_{12}Sb_4S_{13}$ formula unit has a molar mass of 1,666.45 g mol^{-1}, and the unit cell has a lattice parameter a = 10.3908 Å and a volume V = 1.12 × 10^{-21} cm^3 (Wuensch, 1964). With two formula units per unit cell, the theoretical density of tetrahedrite is therefore 4.93 g cm^{-3}.

Although tetrahedrite exists as a body-centered cubic system at room temperature, it also demonstrates a structural phase transition at low-temperature. For many years, various groups recognized through electrical conductivity, heat capacity, and magnetic susceptibility measurements that a metal-semiconductor transition (MST) existed in $Cu_{12}Sb_4S_{13}$ around 85 K (Di Benedetto et al., 2005a; Suekuni et al., 2012; Kitagawa et al., 2015; Suzuki et al., 2015; Nasonova et al., 2016a). Several mechanisms were proposed to explain the physical origin of this MST, including Jahn-Teller distortion or an antiferromagnetic-paramagnetic transformation. However, two recent studies suggested that a cubic-tetragonal phase transition also occurs near 85 K. May et al. utilized temperature-dependent powder X-ray diffraction (XRD) to study the first-order crystallographic transformation (May et al., 2016). Around the same time, Tanaka et al. rigorously analyzed the relationship between physical properties and structure above and below the transition temperature (Tanaka et al., 2016). Additionally, numerous studies have shown that the phase transition is suppressed by the addition of dopants or isovalent substitutions (May et al., 2016; Tanaka et al., 2016; Kosaka et al., 2017). These findings

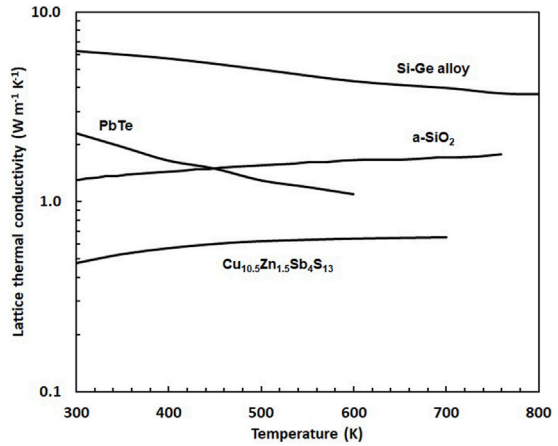

FIGURE 5 | The lattice thermal conductivity of tetrahedrite (typified here by the compound of composition $Cu_{10.5}Zn_{1.5}Sb_4S_{13}$ (Lu et al., 2013);) compared to the lattice thermal conductivity of amorphous silica (Cahill and Allen, 1994), an 70%Si-30% Ge alloy (Abeles et al., 1962), and PbTe (Parashchuk et al., 2021).

support the claim that chemical mutations effectively stabilize the cubic tetrahedrite phase. In this way, the interesting low-temperature behavior of tetrahedrite materials could provide important fundamental information for understanding this class of materials and related systems.

4 LATTICE DYNAMICS AND IMPLICATIONS FOR LATTICE THERMAL CONDUCTIVITY

As previously discussed, a main challenge in thermoelectric materials design is the discovery and development of materials that are good electrical conductors but poor conductors of heat. By the middle of the 20th century, a "tried and true" approach to thermoelectric materials development relied on using solid solutions of semiconductors that comprise heavy mass atoms, while simultaneously possessing a high enough charge carrier mobility to provide good electrical conductivity. These rather stringent requirements, of course, severely limited the choice of available materials for thermoelectrics, and those materials identified early on (e.g., PbTe and Bi_2Te_3) remained the standard bearers throughout the 20th century, and indeed up to the present time. Slack's introduction of the aforementioned "phonon-glass-electron-crystal" concept in 1995 (Slack and Rowe, 1995) together with new ideas in nanostructuring (Dresselhaus et al., 2007) reinvigorated the field and opened the door to much new research.

Tetrahedrite is desirable as a TE material, particularly due to its exceptionally low lattice thermal conductivity (k_l), which approaches the minimum value predicted by theory. This is clearly seen in the comparison of tetrahedrite with Si-Ge alloys, PbTe, and amorphous silica (**Figure 5**). This "minimal" lattice thermal conductivity behavior is partially a consequence of the large $Cu_{12}Sb_4S_{13}$ primitive unit cell volume, which causes a low k_L via low specific heat, and the large number of atoms within the primitive unit cell gives rise to additional optical phonon modes (Morelli and Uher, 2017). Phonon dispersion calculations of $Cu_{12}Sb_4S_{13}$ by Lu et al. (Lu et al., 2013) reveal that the transverse acoustic branches yield a high Grüneisen parameter ($\gamma > 10$) at the zone boundaries, and the three harmonically unstable optical phonon branches are associated with out-of-plane motions of Cu12e atoms. The significant lattice anharmonicity and rattler-like motion of the Cu12e atoms give rise to strong phonon-phonon scattering.

The motion of the three-fold coordinated Cu atom is a key feature of the vibrational density of states (VDOS) in tetrahedrites. The Cu12e has been shown to vibrate with a significantly larger atomic displacement parameter relative to the other atoms (Pfitzner et al., 1997; Lu et al., 2013; Suekuni et al., 2013; Chetty et al., 2015a; Lai et al., 2015). Bonding asymmetry leads to a double-well potential minima where the trigonal Cu atom energetically prefers a slightly out-of-plane position. With a recent fervor, the energetics of the rattling Cu12e atom have been explored by both computational and experimental means (Lara-Curzio et al., 2014; Zhou et al., 2014; Bouyrie et al., 2015a; Li et al., 2016; May et al., 2016; Mishra et al., 2017; Ghassemi et al., 2018; Li et al., 2018; Suekuni et al., 2018) The calculated VDOS for the different atoms in $Cu_{12}Sb_4S_{13}$ (Lai et al., 2015) exhibits a marked low-energy, large-amplitude vibrational mode of the Cu12e atom around 4 meV. This vibrational mode acts as a site that strongly interacts with acoustic phonons, which are the primary heat carriers in the material. Hence, the significant intrinsic phonon scattering seen in tetrahedrites is closely related to the out-of-plane motion of the Cu12e atom.

The origin of the lattice anharmonicity and bonding asymmetry in tetrahedrites is linked to the chemically active Sb lone pairs in the crystal structure. A variety of compounds, including many ternary and quaternary Cu chalcogenides, have been studied to examine the influence of lone pairs in reducing k_L (Skoug and Morelli, 2011; Nielsen et al., 2013; van Embden et al., 2013; Dong et al., 2015; Li et al., 2015; Vaqueiro et al., 2015; Du et al., 2016; Du et al., 2017). In 2015, Lai et al. demonstrated the importance of Sb lone pairs in engendering low k_L in tetrahedrite (Lai et al., 2015). It is as if lone pairs push the Cu12e atom off-center such that it exists in two equally probable locations, and the distorted coordination resembles an off-center trigonal bipyramid (denoted by the space group 48 h). To further justify this visualization, a recent study showed that lone pairs stress the lattice through nearest-neighbor interactions, and the Cu rattling is a way that the structure "retreats" from stress (Suekuni et al., 2018). Again, computational tools have unlocked new possibilities for understanding the lattice dynamics of tetrahedrite materials. Therefore, the Sb lone pair is an essential characteristic that causes tetrahedrite to have a high thermal resistance.

5 ELECTRONIC STRUCTURE

The valence states of different atoms in the tetrahedrite structure are not well-understood by the community, and several models have been proposed over the past 50 years. From a crystal

chemistry perspective, a distribution of two Cu^{2+} and ten Cu^{1+} atoms would satisfy charge-balance (Cu_{10}^{1+} Cu_{2}^{2+} Sb_{4}^{3+} S_{13}^{2-}) (Wuensch, 1964). This model assumes ionic bonding character and predicts that the two Cu^{2+} atoms strictly occupy tetrahedral 12 d sites. However, Cu-based tetrahedrites are stable over a large compositional range up to the $Cu_{14}Sb_4S_{13}$ and $Cu_{12}Sb_{4.67}S_{13}$ end-members, and in turn, a Brillouin-zone (BZ) model of valence electron counting was proposed. In the BZ model, a window of stability is allowed for tetrahedrite compositions with 204–208 valence electrons (Johnson and Jeanloz, 1983; Jeanloz and Johnson, 1984). In this model for the electronic structure of tetrahedrite, the total number of valence electrons per unit cell are accounted for. All copper atoms are taken to be in the monovalent Cu^{1+} state. Transition metal substituents such as Zn are assumed to be in the divalent (2+) state, whereas Sb is assumed to be trivalent and each sulfur atom provides six electrons. Thus, in the context of this BZ electron-counting scheme, one moves from 204 to 208 electrons per unit cell, respectively, in going from $Cu_{12}Sb_4S_{13}$ to $Cu_{10}Zn_2Sb_4S_{13}$. Whether a particular composition of tetrahedrite is semiconducting or metallic will be determined by whether the last BZ to be filled is completely or partially full. For 204 electrons, the last (51st) BZ is completely filled, whereas for 208 electrons the last (52nd) BZ is completely filled, since each BZ can accommodate up to four electrons. Experimentally, EPR measurements on synthetic $Cu_{12}Sb_4S_{13}$ (Di Benedetto et al., 2005b) reveal that some copper atoms are in a mixed-valent or pseudo-divalent state between 1+ and 2+. In this picture, then, $Cu_{12}Sb_4S_{13}$ is not a true semiconductor but rather exhibits metallic behavior, in agreement with experimental studies. Another interesting implication of the BZ model is that the pseudo-divalent Cu atoms can exhibit mobility in the structure and thus contribute to ionic conduction (Vaqueiro et al., 2017), obviously a serious drawback in and thermoelectric application. Interestingly though, substitution of these divalent Cu atoms with transition metals such as Zn seems to have the effect of suppressing the ionic conductivity (Mozgova et al., 1987). It is thought that the divalent transition metals occupy previously empty tetrahedral sites and thus block the ionic conductivity pathway. It is not by coincidence, then, that natural mineral samples do not exhibit ionic conductivity, as some transition metal content on the Cu site is always found in them.

Pattrick *et al.* offered further support for the BZ model by using X-ray absorption spectroscopy to show that the ratio of Cu^{1+} to Cu^{2+} is dependent on chemical composition (Pattrick et al., 1993). Contrary to this model, density-functional theory (DFT) calculations, complemented by experimental data, have provided evidence to suggest that all of the Cu atoms could maintain a monovalent state (Lu et al., 2013). This claim is also justified by high ionic conductivity and mixed ionic/covalent bonding observed in tetrahedrites (Lai et al., 2015). Accordingly, modern computational tools have enabled a novel approach for understanding atomic valence states in tetrahedrites, but there is still much more to be learned.

Cu-based tetrahedrite behaves like a metal with p-type conductivity. In 2013, Lu *et al.* calculated the electronic band structure and electronic density of states (EDOS) of tetrahedrite via DFT (Lu et al., 2013). Since then, multiple other groups have made similar calculations (Suekuni et al., 2013; Tablero, 2014; Zhou et al., 2014). In $Cu_{12}Sb_4S_{13}$, the valence band is primarily a result of hybridization between Cu 3 d and S 3p orbitals, where all elements contribute equally to the conduction band. The indirect band gap is approximately equal to 1.1 eV, and the Fermi level (E_F) resides in the VB near the band edge. By replacing Cu^{1+} with Zn^{2+}, E_F rises into the gap and the sample becomes insulating. One can think of $Cu_{12}Sb_4S_{13}$ as a dirty metal, whereas $Cu_{10}Zn_2Sb_4S_{13}$ is the true semiconducting composition. In both cases, Hall measurements provide only a small signal, making determination of hole concentration and mobility difficult (Lu et al., 2013; Tippireddy et al., 2018a). Regardless, doping and substituting different atoms into the tetrahedrite structure may be used to manipulate its properties in a favorable way.

In contrast to Zn, for which in the divalent state the d-band is completely full, other transition metal dopants such as Ni and Fe have a d-band that is partially occupied, and this leads to some interesting exchange splitting effects. The band structure of several of these has been investigated theoretically (Lu et al., 2013; Suekuni et al., 2013; Heo et al., 2014; Suekuni et al., 2014; Chetty et al., 2015a). For the case of Ni doping, for example, while the majority spin states are fully occupied, the minority spin states exist as three acceptor-like bands lying above the Fermi level. These are partially filled and therefore engender a finite density of states at the Fermi level. The implication of this is that for substitutions of Ni up to even x = 2, the compound remains metallic, unlike the case for Zn substitution; this has been confirmed experimentally (Suekuni et al., 2013).

For the case of Mn substituting for Cu, the majority spin state is occupied and the minority spin state unoccupied. The latter, however, is situated in the conduction band of the host, and thus far removed from the valence band. For this reason, Mn-doped tetrahedrite, like Zn, approaches an insulating state for x = 2 (Chetty et al., 2015a).

Finally, the case of Fe-doping is an especially interesting one. Using Mössbauer spectroscopy techniques, Makovicky and coworkers (Makovicky et al., 1990) demonstrated that for $0 < x < 1$ in synthetic $Cu_{12-x}Fe_xSb_4S_{13}$, Fe occurs in the ferric (3+) state, while for $1 \leq x \leq 2$ it is in the ferrous (2+) state. Therefore, at low Fe concentrations, each Fe has one extra electron, compared to Zn, to fill holes in the valence band. This has been confirmed by DFT calculations, which show that for $Cu_{11}FeSb_4S_{13}$ the iron ions are in a Fe^{3+} s^0d^5 configuration (Lu et al., 2013).

6 THERMOELECTRIC PROPERTIES

Within the past few years, TE research has gained significant momentum with respect to tetrahedrite and its many variants. **Figure 6** summarizes the optimized *zT* values obtained for tetrahedrite TEs previously. To the best of the authors' knowledge, these studies have reported *zT* data for tetrahedrites, with almost all the high-temperature studies achieving values above 0.6 from 673 to 723 K. Moreover,

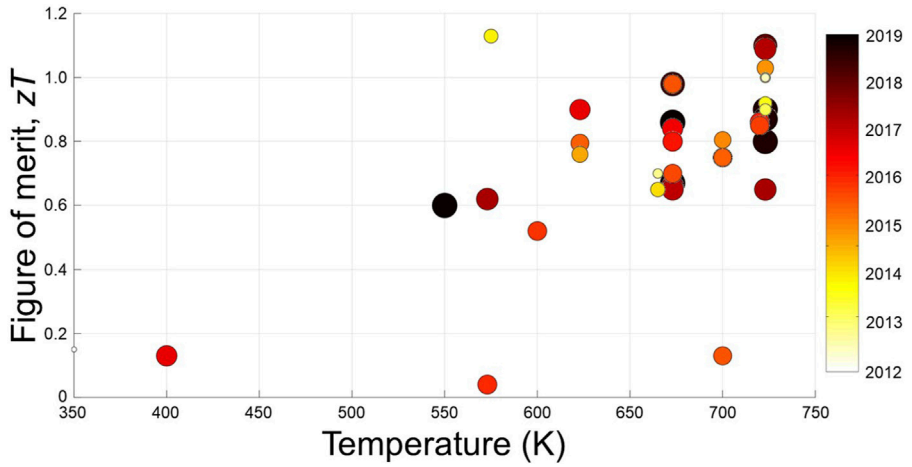

FIGURE 6 | Scatter plot summarizing peak figure of merit values for tetrahedrite-based materials obtained from 38 primary research reports since 2012. To enhance visual clarity, data markers are color coded and scaled by size according to publication year (i.e., darker/larger markers are data from more recent studies).

several of these materials reached zT beyond unity above 673 K. The two outlier data points, which exhibit low figures of merit even at high temperatures, are natural mineral tetrahedrite specimens. As a result, impurities lead to low TE performance in these samples. Conversely, some previous studies have achieved zT near unity by mixing natural mineral tetrahedrites with a purely synthetic seed phase (Lu and Morelli, 2013a; Lu and Morelli, 2013b). Overall, tetrahedrites have been researched for their TE properties steadily since 2012, with even more studies focusing on other interesting phenomena in these fascinating materials. Most of the compounds in **Figure 6** will be mentioned in the following subsections. First, the typical Cu-based compositions will be discussed, along with Cu-enriched samples. Then, doped and substituted compounds will be covered.

6.1 Cu-Based Tetrahedrites

Cu-based tetrahedrites were some of the first compositions to be examined for TE applications, and they served as a foundational model system for future studies. In 2012, Suekuni et al. was the first to report TE properties of $Cu_{12}Sb_4S_{13}$ (Suekuni et al., 2012). Not long after, numerous investigations obtained zT values up to 0.5 at 673 K for the unsubstituted composition. (Abeles et al., 1962; Pattrick et al., 1993; Cahill and Allen, 1994; Lu et al., 2013). More recent studies reported even higher ZT values as the process optimization for this system became more well-understood. (Pattrick et al., 1993; Lu et al., 2015; Prem Kumar et al., 2016a; Wang et al., 2016; Sun et al., 2017; Kim et al., 2019a). Unfortunately, the majority of these studies present data from samples containing impurity phases of famatinite (Cu_3SbS_4), skinnerite (Cu_3SbS_3), chalcostibite ($CuSbS_2$), copper sulfides ($Cu_{2-x}S$), or elemental Sb. Specifically, famatinite is a very common secondary phase that easily forms when synthesizing Cu-based tetrahedrites, and more often than not, TE studies of $Cu_{12}Sb_4S_{13}$ report data for samples that contain Cu_3SbS_4. Accordingly, while Cu-based tetrahedrite demonstrates good TE properties, it also has a propensity for forming impurity phases.

Cu-rich tetrahedrites have garnered significant attention in recent years. Although the nominal composition of tetrahedrite is denoted by $Cu_{12}Sb_4S_{13}$, the precise elemental composition and atomic distribution can vary to a large degree. For instance, Cu-based tetrahedrite stoichiometries can range from Cu-poor ($Cu_{12}Sb_4S_{13}$) to Cu-rich ($Cu_{14}Sb_4S_{13}$). The compositional variations in Cu-based tetrahedrites were studied by mineralogists and geologists well before the material was ever tried for TE applications (Tatsuka and Morimoto, 1973; Tatsuka and Morimoto, 1977; Johnson et al., 1988). In Cu-rich tetrahedrites, Cu12d sites are partially vacated and extra Cu ions reside in interstices of the lattice, creating a network of vacant tetrahedral and interstitial sites (Makovicky and Skinner, 1979; Vaqueiro et al., 2017). It is believed that this network enables high Cu ion mobility in tetrahedrites. The enhanced ionic conductivity of Cu ions leads to an exsolution of two immiscible tetrahedrite phases (Cu-poor and Cu-rich). Only recently were Cu-rich tetrahedrites investigated for their TE capabilities.

In 2017, Vaqueiro et al. measured the properties of $Cu_{12+x}Sb_4S_{13}$ ($0 \leq x \leq 2$) and examined the onset of Cu ion mobility as a function of temperature (Vaqueiro et al., 2017). It was also shown that the phase segregation in Cu-rich samples significantly reduced k_L. More recently, Yan et al. analyzed the properties of Cu-rich tetrahedrites, obtaining $k_L = 0.25$ W m^{-1}K^{-1} and $zT = 1$ at 723 K for $Cu_{13.5}Sb_4S_{13}$ (Yan et al., 2018). In the end, both studies demonstrated that Cu-enrichment can lead to greater zT values, primarily through a reduction in k_L. Kim, et al. (Kim et al., 2019a) explored mechanical alloying and hot pressing of $Cu_{12}Sb_4S_{13}$ and

showed that this composition exhibited weight loss at temperatures above 853 K, likely due to decomposition and melting. Optimized samples reached a zT value of 0.87 at 723 K.

6.2 Doped and Substituted Tetrahedrites

The massive compositional variation allowed by the tetrahedrite crystal structure has enabled a multitude of TE investigations of various doped and substituted samples. To begin with, a wide variety of transition metals may replace Cu atoms in the structure, and such replacements have been observed in natural mineral tetrahedrites (Johnson et al., 1986). Initially, Suekuni et al. measured TE properties of transition metal (M = Mn, Fe, Co, Ni, Cu, and Zn) substituted tetrahedrites ($Cu_{10}M_xSb_4S_{13}$) up to the substitutional limit (x = 2) (Suekuni et al., 2012). In the end, $Cu_{10}Ni_2Sb_4S_{13}$ demonstrated the best zT of all the samples reaching a maximum value of 0.15 at 340 K. Soon after, this group and another group reported TE properties for substituted tetrahedrites at higher temperatures. (Lu et al., 2013; Suekuni et al., 2013). These and other studies were guided by modern computational simulations that investigated the electronic properties of doped tetrahedrites (Lara-Curzio et al., 2014; Tablero, 2014; Zhou et al., 2014; Kim et al., 2019a; Pi et al., 2019). As discussed previously, E_F lies at the valence band edge for the Cu-based composition, and adding Zn atoms, which strictly adopt a divalent state, effectively raises E_F into the gap. Accordingly, Zn acts as a dopant by contributing extra electrons to the lattice. By leveraging this knowledge, Lu et al. demonstrated the first zT near unity for Zn-doped tetrahedrite ($Cu_{11.5}Zn_{0.5}Sb_4S_{13}$) at 723 K (Dong et al., 2021). Therefore, simple replacements of Cu with 3 d transition metals laid the groundwork for future TE studies with tetrahedrites.

Since the early TE investigations of doping in tetrahedrite, a plethora of studies have been published for tetrahedrites doped with 3 d transition metals (Tippireddy et al., 2018a). Structural, magnetic, and TE research analyzed dopants like Mn (Chetty et al., 2015a; Coelho et al., 2020), Fe (Andreasen et al., 2008; Lu et al., 2013; Chetty et al., 2015b; Nasonova et al., 2016b; Guler et al., 2016), Co (Barbier et al., 2015a; Bouyrie et al., 2016a; Kim et al., 2019b; Kim et al., 2020), Ni (Suekuni et al., 2013; Lara-Curzio et al., 2014; Barbier et al., 2016; Bouyrie et al., 2016b; Gonçalves et al., 2016), Zn (Lara-Curzio et al., 2014; Barbier et al., 2015b; Harish et al., 2016), Al (Tippireddy et al., 2020), Gd (Zhu et al., 2021), Mg (Levinsky et al., 2019) and Cd (Prem Kumar et al., 2016a) in synthetic tetrahedrites. One of the highest zT values reported to date is that of Lu et al., which reached $zT = 1$ at 720 K for Ni and Zn co-doped tetrahedrite ($Cu_{10.5}Ni_1Zn_{0.5}Sb_4S_{13}$) (Lu et al., 2015). Aside from enhancements in zT, these studies seem to indicate that dopants mitigate the formation of impurity phases. In fact, two studies showed explicitly that the tetrahedrite phase preferentially forms over other secondary phases when small amounts of dopant are present in the structure (Seal et al., 1990; Barbier et al., 2015b). Over the years, numerous studies have echoed a similar observation (Tatsuka and Morimoto, 1973; Di Benedetto et al., 2002). Thus, a vast collection of studies have shown that zT can be greatly improved by doping and substituting with 3 d transition metals, while also stabilizing the primary tetrahedrite phase in these samples and suppressing ionic conductivity effects.

Although many studies have examined transition metal substitution in tetrahedrites, the complexity of the crystal structure allows for more exotic dopants, aside from 3 d transition metals. For instance, Ge and Sn doping were recently explored, exhibiting a compositional limit of about x = 0.6 in $Cu_{12-x}(Ge, Sn)_xSb_4S_{13}$ (Kosaka et al., 2017). On another note, Ag (Pattrick and Hall, 1983) and Au (Zazakowny et al., 2022) substitution has been shown to be possible in synthetic tetrahedrites, and Pb doping ($Cu_{11}PbSb_4S_{13}$) demonstrated zT enhancements of about 40% at 723 K when compared to Cu-based compositions (Huang et al., 2018). Regardless of the cost-effectiveness and toxicity of these tetrahedrites, these studies are evidence that multitudinous elemental substitutions have yet to be explored. Hence, a copious variety of elements, in addition to 3 d transition metals, may be used as dopants on the Cu site in tetrahedrite, and there are many such compositions that have not been reported in the literature.

The inclusion of dopants on Sb sites has also been studied, and in certain cases, large improvements to TE performance were observed. To begin with, Lu and Morelli synthesized $Cu_{12}Sb_{4-x}Te_xS_{13}$ ($0 \leq x \leq 1.5$), and a peak zT value of 0.92 was obtained at 723 K for x = 1 (Lu and Morelli, 2014). These workers surmised that tetravalent Te atoms substituting for trivalent Sb provided electrons to fill valence band holes, similar to the effect of Zn substituting for Cu. Following this study, Bouyrie and coworkers explored Te substitution and multi-site doping with transition metals (Cu site) and Te (Sb site) (Chetty et al., 2015a; Bouyrie et al., 2015b; Chetty et al., 2015b; Bouyrie et al., 2015c; Barbier et al., 2016). Kwak et al. (Kwak et al., 2021) also successfully doped with Te on the Sb site and achieved a zT of 0.8 at 723 K. In addition, doping the Sb site with Bi has been shown to yield zT of 0.84 at 673 K in $Cu_{12}Sb_{3.8}Bi_{0.2}S_{13}$ (Prem Kumar et al., 2016b). A similar value of zT was obtained for Bi-doped samples by Kwak, *et al.* (Kwak et al., 2020) using a mechanical alloying and hot-pressing approach. Tippireddy, et al. (Tippireddy et al., 2019) attempted Sn doping on the Sb site, and found that Sn substituted for both Sb and Cu in the structure. Very recently, Ahn and Kim (Ahn and Kim, 2021) reported successful doping of Sn on the Sb site with $zT = 0.66$ for $Cu_{12}Sb_{3.9}Sn_{0.1}S_{13}$. Finally, As substitution for Sb is also possible in synthetic tetrahedrites (Guler et al., 2016), of course, which just mimics the well-known tetrahedrite-tennantite solid solution that occurs in natural minerals. Accordingly, some compositional variation exists on the Sb site, which has been utilized to improve zT in certain tetrahedrites.

Lastly, S site modifications in tetrahedrite materials have been researched within the last few years as well. Tetrahedrite compositions with Se and Te as anions were examined in early mineralogical studies, and more recently, computational simulations predicted stable phases of the tetrahedrite structure with Se as the chalcogenide (Moller and Makovicky, 1999; Zhang et al., 2014). In 2016, a solid solution of $Cu_{12}Sb_4S_{13-x}Se_x$ ($0 \leq x \leq 2$) was synthesized, and a maximum zT of 0.84 was obtained at 720 K for the x = 1 composition (Lu et al., 2016). For these Se substituted

compounds, researchers attribute improvements in zT to reduced k_L, due to increased alloy scattering of phonons. Subsequently, Cu-enrichment in $Cu_{12+x}Sb_4S_{12}Se$ provided even greater boosts to TE performance, obtaining zT of approximately 1.1 at 723 K for the $Cu_{13.5}Sb_4S_{12}Se$ composition (Yan et al., 2018). To the authors' knowledge, this is the highest ZT reported to date for all tetrahedrite compounds. Finally, a recent study involving multi-site doping with Zn and Se in tetrahedrites was conducted and the TE properties investigated, and an optimized zT of 0.86 was demonstrated at 673 K for $Cu_{11}ZnSb_4S_{12.75}Se_{0.25}$ (Tippireddy et al., 2018b). In the end, isovalent Se substitution in tetrahedrites has been shown to benefit TE properties, especially in combination with other chemical modifications.

7 MECHANICAL PROPERTIES

The mechanical properties of thermoelectric materials are important for ensuring long operating lifetimes. As materials undergo heat transfer processes, they experience thermal expansion and thermal stress. In order to minimize thermal stress, small values of Young's modulus, linear thermal expansion coefficient, and Poisson's ratio are required at a fixed temperature gradient. Early work was done by Fan et al. to measure hardness, Young's modulus, shear modulus, Poisson's ratio, and bulk modulus in synthetic and natural mineral tetrahedrites (Fan et al., 2013). In terms of thermal stress, they found that tetrahedrite had similar or advantageous properties over other TE materials like PbTe, SiGe, and $CoSb_3$. These results support longer lifetimes in thermoelectric devices made from tetrahedrites because they can undergo many thermal cycles without mechanical degradation. On the other hand, due to its anharmonic bonding nature, tetrahedrite has a fracture toughness of 0.47 MPa, which is similar to PbTe and much lower than other materials (Fan et al., 2013). However, tetrahedrites have a brittle index similar to other TE materials as well, indicating desirable qualities for machinability. Therefore, tetrahedrite has mechanical properties comparable to other state-of-the-art TEs with a strong resistance to thermal stress, good machinability, but a relatively poor fracture toughness.

Several other studies have involved characterizing the mechanical properties of tetrahedrites. For example, Sun et al. investigated brittleness, thermal stability, and microstructure in tetrahedrites (Sun et al., 2017). Ultimately, their results indicated that mechanical properties can be improved with additional spark plasma sintering processing, beyond what conventional syntheses require. Barbier et al. used DSC and TGA to examine the thermal stability of Cu based and Ni doped tetrahedrites (Barbier et al., 2015b). They found that Cu based tetrahedrite decomposed into Cu_3SbS_3 at 791 K, but this decomposition temperature was raised significantly in the Ni doped tetrahedrite. Thus, impurity substitution leads to a stabilization of the compound and raise its maximum operating temperature. Lastly, Pi et al. studied the mechanical properties of tetrahedrites after thermal aging in air and vacuum (Pi et al., 2019). They reported values for the Vickers hardness and bending strength of copper-based tetrahedrites. All in all, mechanical issues impede the application of tetrahedrite materials on a widespread scale, and there is still room for fruitful research involving mechanical characterization of doped and undoped tetrahedrites.

8 RAPID AND FACILE SYNTHESIS METHODS

The substantial majority of tetrahedrite studies utilize a traditional melt-recrystallization approach. In this approach, elemental precursors are loaded into a quartz ampoule with subsequent evacuation and heating to 650°C with a hold time of at least 12 h (Lu and Morelli, 2013a). A slow heating rate (0.3°C min^{-1}) is a necessary precaution for preventing pressure build-up from volatilized S. The resultant ingot does not come out phase-pure, and in turn, it is subsequently ground, pressed, and annealed for up to 3°weeks at 450°C. Finally, the sample is ground and consolidated via either hot-pressing or spark plasma sintering. Overall, long reaction times (12–40 + h), accompanied by a lengthy annealing phase (25 h–3 weeks), are required to promote the formation of single-phase tetrahedrite by this method. Due to long synthesis times and high energy requirements, the melt-recrystallization approach is not amenable to large-scale applications. Therefore, faster and less energy-intensive techniques than the traditional approach would be more favorable for commercial application of tetrahedrite materials.

8.1 Mechanical Alloying

Mechanical alloying is a straightforward technique, where powder precursors undergo a mechanochemical reaction *via* milling. The grinding media, milling time, and atmospheric reactivity are common factors to consider when performing these reactions. Since the 1990s, mechanical alloying research has gained momentum in an effort to find viable industrial alternatives to rapid solidification processing reactions (Suryanarayana et al., 2001). A diverse array of materials are viable candidates for mechanical alloying synthesis, including intermetallic compounds and ceramics oxides (Al-Joubori and Suryanarayana, 2015; Gondim et al., 2015). Commonly, powderized products from the milling process are densified by hot-pressing or spark plasma sintering (SPS).

Several groups have synthesized tetrahedrites by mechanical alloying. Barbier and coworkers were the first group to do this by synthesizing $Cu_{10.4}Ni_{1.6}Sb_4S_{13}$ and obtaining zT of 0.75 at 700 K (Barbier et al., 2015a). In a follow-up study by the same group, the scalability of this procedure was utilized for fabricating large square monoliths (50 × 50 × 3 mm) of tetrahedrite from mechanically alloyed powders (Barbier et al., 2016). Similarly, Harish et al. studied phase stability in Zn-doped tetrahedrites made by mechanical alloying (Bouyrie et al., 2016b). More recently, $Cu_{12}Sb_4S_{13}$ was prepared by planetary milling at 350 rpm for 24 h (Kim et al., 2019a). To the authors' knowledge, this study provided the highest zT to date for the unsubstituted composition, reaching a peak zT of 0.87 at 723 K. In another study, $Cu_{12}Sb_4S_{13}$ was synthesized by mechanical

alloying for photovoltaic thin film applications (Prem Kumar et al., 2018). Weller and Morelli (Weller and Morelli, 2017) also used a combined mechanical alloying/spark plasma sintering approach to produce Ni/Zn co-doped specimens and achieved a maximum zT value of 0.66 at 673 K for optimized compositions. Therefore, mechanical alloying has been shown to be a practical approach for producing tetrahedrite TE materials.

8.2 Reactive SPS

Reactive SPS is a method that rapidly synthesizes materials in a single step. Whereas other approaches trivially use SPS for powder processing, a chemical reaction takes place in addition to consolidation in the reactive approach. In general, SPS is relatively novel technique with much of the technological development and applied research occurring after the year 2000 (Guillon et al., 2014). "Spark plasma sintering" is somewhat of a misnomer, since no spark is actually detectable from this method; in turn, many researchers have used the terms "field-assisted sintering technique" or "pulsed electric current sintering" instead (Hulbert et al., 2008). In particular, reactive SPS is useful for working with ultra-high temperature ceramics, which require reaction temperatures that are otherwise difficult to reach by means of traditional furnace heating (Orrù and Cao, 2013). Previously, reactive SPS has been used for the synthesis of composites and a variety of borides, carbides, nitrides, oxides, and silicides (Wang et al., 2004; Wu et al., 2007; Zhao et al., 2007; Locci et al., 2009; Sahin et al., 2012; Sun et al., 2013; Karthiselva et al., 2015) As a result, this approach has been used for a wide range of applications in materials science. Nanocrystalline materials especially benefit from SPS methods because the rapid nature of the sintering process mitigates grain coarsening.

Numerous groups have used SPS for densification of tetrahedrite materials, but there are very few studies using sintering as a synthetic approach for forming tetrahedrites. Battiston et al. published a one-step sintering synthesis for Ni and Zn substituted tetrahedrites. They used open die pressing as a fast and simple method for obtaining doped tetrahedrites in less than 6 h. It should also be noted that their Ni substituted samples exhibited secondary phases of NiSbS and Cu_2S. In the end, the best zT for Ni and Zn co-doped tetrahedrites prepared by open die pressing was 0.65 at 673 K for $Cu_{11}NiZnSb_4S_{13}$ (Battiston et al., 2017). Weller and Morelli (Weller and Morelli, 2017) employed the reactive SPS technique using binary sulfide precursors which utilized a short ball milling step followed by reactive spark plasma sintering to form tetrahedrite, the entire process requiring less than 2 h of total synthesis time.

8.3 Solution-Phase Synthesis

Solution-phase synthesis methods boast many advantages over the conventional melt-crystallization synthesis, but these techniques possess their own drawbacks as well. While the "top-down" melt-recrystallization approach requires high temperatures and long reaction times, "bottom-up" methodologies may be preferable because they often yield nanostructured material and require lower temperatures and shorter synthesis times. Previously, Cu-Sb-Se-S nanomaterials have been synthesized by a variety of wet-chemical approaches, such as hot-injection (Ramasamy et al., 2014; Chen et al., 2015; Suehiro et al., 2015; Wu et al., 2015; Chen et al., 2016; Bera et al., 2018) or solvothermal (An et al., 2003; James et al., 2015; John et al., 2018) synthesis. Most notably, James et al. achieved zT = 0.63 at 720 K for $Cu_{12}Sb_4S_{13}$ synthesized by the solvothermal method (James et al., 2015). In a different study, the optical properties and charge generation capabilities of tetrahedrite thin films prepared from metal xanthates were examined (Rath et al., 2015). Weller, et al. (Weller et al., 2017) used a modified polyol process to synthesize pure and Zn-doped tetrahedrite powders, and pellets consolidated by SPS from these powders were found to have zT values comparable to, if not exceeding, those made using solid state methods. In another study, this same group employed the identical process to synthesize Fe-doped tetrahedrites (Weller et al., 2018). A notable outcome of this study was the observation of n-type behavior for certain Fe compositions, although this occurred only below room temperature. It was suggested that this behavior, to the authors' knowledge the only report of n-type tetrahedrite, was related to the presence of mixed valence Fe^{2+}/Fe^{3+} in these samples.

Unfortunately, these solution-phase techniques commonly yield product on the scale of ~100 mg per batch, and multiple batches must be combined to obtain enough material for TE characterization. Furthermore, wet-chemical approaches pose a greater risk of contamination because they often require careful removal of undesirable byproducts. Lastly, nanoscale materials demonstrate higher reactivity due to their increased surface energy, and as a result, organic additives (i.e., ligands or surfactants) are usually employed to stabilize the material. However, previous studies provide evidence to suggest that organics can be detrimental to TE performance (Stavila et al., 2013). Therefore, solution-phase syntheses require shorter reaction times and less energy-intensive processes, but they typically utilize organics for stability and only produce small amounts of material in each batch.

To summarize, an array of facile and rapid synthesis techniques has been employed to create high performance tetrahedrite thermoelectric materials. It is a remarkable feature of the tetrahedrite system that it seems to be very robust with respect to consistently displaying zT values between 0.5 and 1.0 for a variety of compositions and processing methods. The potential low cost and ease of use of these facile synthesis approaches Bode well for their implementation in large-scale thermoelectric power generation applications.

8 SUMMARY

As an ever more energy-hungry globe struggles with limited energy supply and increasing energy demand, energy usage on planet Earth will continue to evolve from fossil-fuel-based to renewables-based. This transition will not be instantaneous, however, and in the interim period (which will no doubt be many years), increasing the efficiency of fossil-fuel utilization and decreasing its impact on the environment must be emphasized. To this end, thermoelectrics can play a leading role in converting

the enormous amount of waste heat created in energetic processes to useful energy. This review has focused on the science and technology of tetrahedrite thermoelectrics, a new class of materials to emerge within the last decade. The unusual crystal structure and bonding in these materials plays an important role in endowing them with their unique thermoelectric properties. The ability to substitute many different elements on all three chemical sites in tetrahedrite has been highlighted here, and it is concluded that thermoelectric figure of merit of tetrahedrites is remarkably robust across a range of chemical compositions. Further, a host of rapid and facile synthesis techniques have been deployed that allow for the straightforward research and development of this material on a large scale. Taken together, all of these factors point to a bright future for the use of tetrahedrites in large-scale power generation and waste heat recovery applications.

AUTHOR CONTRIBUTIONS

DM and DW contributed equally to this manuscript.

REFERENCES

Abeles, B., Beers, D. S., Cody, G. D., and Dismukes, J. P. (1962). Thermal Conductivity of Ge-Si Alloys at High Temperatures. *Phys. Rev.* 125, 44.

Abeles, B. (1963). Lattice Thermal Conductivity of Disordered Semiconductor Alloys at High Temperatures. *Phys. Rev.* 131, 1906–1911. doi:10.1103/physrev.131.1906

Ahn, H. J., and Kim, I. H. (2021). Charge Transport and Thermoelectric Properties of Sn-Doped Tetrahedrites Cu12Sb4-ySnyS13. *Korean J. Met. Mat.* 59, 736. doi:10.3365/kjmm.2021.59.10.736

Akhiezer, A. (1940). The Thermal Conductivity of Nonmetallic Crystals. *Zh. Eksp. Teor. Fiz.* 10, 1354.

Al-Joubori, A. A., and Suryanarayana, C. (2015). Synthesis of Metastable NiGe2 by Mechanical Alloying. *Mater. Des.* 87, 520–526. doi:10.1016/j.matdes.2015.08.051

An, C., Jin, Y., Tang, K., and Qian, Y. (2003). Selective Synthesis and Characterization of Famatinite Nanofibers and Tetrahedrite Nanoflakes. *J. Mat. Chem.* 13, 301–303. doi:10.1039/b210703a

Andreasen, J. W., Makovicky, E., Lebech, B., and Møller, S. K. (2008). The Role of Iron in Tetrahedrite and Tennantite Determined by Rietveld Refinement of Neutron Powder Diffraction Data. *Phys. Chem. Miner.* 35, 447–454. doi:10.1007/s00269-008-0239-1

Barbier, T., Lemoine, P., Gascoin, S., Lebedev, O. I., Kaltzoglou, A., Vaqueiro, P., et al. (2015). Structural Stability of the Synthetic Thermoelectric Ternary and Nickel-Substituted Tetrahedrite Phases. *J. Alloys Compd.* 634, 253–262. doi:10.1016/j.jallcom.2015.02.045

Barbier, T., Lemoine, P., Martinet, S., Eriksson, M., Gilmas, M., Hug, E., et al. (2016). Up-scaled Synthesis Process of Sulphur-Based Thermoelectric Materials. *RSC Adv.* 6, 10044–10053. doi:10.1039/c5ra23218j

Barbier, T., Rollin-Martinet, S., Lemoine, P., Gascoin, F., Kaltzoglou, A., Vaqueiro, P., et al. (2015). Thermoelectric Materials: A New Rapid Synthesis Process for Nontoxic and High-Performance Tetrahedrite Compounds. *J. Am. Ceram. Soc.* 99, 51–56. doi:10.1111/jace.13838

Battiston, S., Fanciulli, C., Fiameni, S., Famengo, A., Fasolin, S., and Fabrizio, M. (2017). One Step Synthesis and Sintering of Ni and Zn Substituted Tetrahedrite as Thermoelectric Material. *J. Alloys Compd.* 702, 75–83. doi:10.1016/j.jallcom.2017.01.187

Bera, S., Dutta, A., Mutyala, S., Ghosh, D., and Pradhan, N. (2018). Predominated Thermodynamically Controlled Reactions for Suppressing Cross Nucleations in Formation of Multinary Substituted Tetrahedrite Nanocrystals. *J. Phys. Chem. Lett.* 9, 1907–1912. doi:10.1021/acs.jpclett.8b00680

Biswas, K., He, J., Blum, I. D., Wu, C.-I., Hogan, T. P., Seidman, D. N., et al. (2012). High-performance Bulk Thermoelectrics with All-Scale Hierarchical Architectures. *Nature* 489, 414–418. doi:10.1038/nature11439

Bouyrie, Y., Candolfi, C., Dauscher, A., Malaman, B., and Lenoir, B. (2015). Exsolution Process as a Route toward Extremely Low Thermal Conductivity in Cu12Sb4-xTexS13 Tetrahedrites. *Chem. Mat.* 27, 8354–8361. doi:10.1021/acs.chemmater.5b03785

Bouyrie, Y., Candolfi, C., Ohorodniichuk, V., Malaman, B., Dauscher, A., Tobola, J., et al. (2015). Crystal Structure, Electronic Band Structure and High-Temperature Thermoelectric Properties of Te-Substituted Tetrahedrites Cu12Sb4−xTexS13 (0.5 ≤ X ≤ 2.0). *J. Mat. Chem. C* 3, 10476–10487. doi:10.1039/c5tc01636c

Bouyrie, Y., Candolfi, C., Pailhes, S., Koza, M. M., Malaman, B., Dauscher, A., et al. (2015). From Crystal to Glass-like Thermal Conductivity in Crystalline Minerals. *Phys. Chem. Chem. Phys.* 17, 1975. doi:10.1039/c5cp02900g

Bouyrie, Y., Candolfi, C., Vaney, J. B., Dauscher, A., and Lenoir, B. (2016). High Temperature Transport Properties of Tetrahedrite Cu12−x M X Sb4−y Te Y S13 (M = Zn, Ni) Compounds. *J. Elec Materi* 45, 1601–1605. doi:10.1007/s11664-015-4128-3

Bouyrie, Y., Sassi, S., Candolfi, C., Vaney, J.-B., Dauscher, A., and Lenoir, B. (2016). Thermoelectric Properties of Double-Substituted Tetrahedrites Cu12−xCoxSb4−yTeyS13. *Dalton Trans.* 45, 7294–7302. doi:10.1039/c6dt00564k

Cahill, D. G., and Allen, T. H. (1994). Thermal Conductivity of Sputtered and Evaporated SiO2and TiO2optical Coatings. *Appl. Phys. Lett.* 65, 309–311. doi:10.1063/1.112355

Callaway, J., and von Baeyer, H. C. (1960). Effect of Point Imperfections on Lattice Thermal Conductivity. *Phys. Rev.* 120, 1149–1154. doi:10.1103/physrev.120.1149

Chen, D., Zhao, Y., Chen, Y., Lu, T., Wang, Y., Zhou, J., et al. (2016). Thermoelectric Enhancement of Ternary Copper Chalcogenide Nanocrystals by Magnetic Nickel Doping. *Adv. Elec. Mat.* 2, 2. doi:10.1002/aelm.201500473

Chen, K., Zhou, J., Chen, W., Zhou, P., He, F., and Liu, Y. (2015). Size-Dependent Synthesis of Cu12Sb4S13Nanocrystals with Bandgap Tunability. *Part. Part. Syst. Charact.* 32, 999–1005. doi:10.1002/ppsc.201500088

Chetty, R., Bali, A., Naik, M. H., Rogl, G., Rogl, P., Jain, M., et al. (2015). Thermoelectric Properties of Co Substituted Synthetic Tetrahedrite. *Acta Mater.* 100, 266–274. doi:10.1016/j.actamat.2015.08.040

Chetty, R., Kumar, P., Rogl, G., Rogl, P., Bauer, E., Herwig, M., et al. (2015). Thermoelectric Properties of a Mn Substituted Synthetic Tetrahedrite. *Phys. Chem. Chem. Phys.* 17, 1727. doi:10.1039/c4cp04039b

Coelho, R., Symeou, E., Kyratsi, T., and Pereira Gonçalves, A. (2020). Tetrahedrite Sintering Conditions: The Cu11Mn1Sb4S13 Case. *J. Elec Materi* 49, 5077–5083. doi:10.1007/s11664-020-08250-3

Di Benedetto, F., Bernardini, G. P., Borrini, D., Emiliani, C., Cipriani, C., Danti, C., et al. (2002). Crystal Chemistry of Tetrahedrite Solid-Solution: Epr and Magnetic Investigations. *Can. Mineralogist* 40, 837–847. doi:10.2113/gscanmin.40.3.837

Di Benedetto, F., Bernardini, G. P., Cipriani, C., Emiliani, C., Gatteschi, D., and Romanelli, M. (2005). The Distribution of Cu(II) and the Magnetic Properties of the Synthetic Analogue of Tetrahedrite: Cu12Sb4S13. *Phys. Chem. Miner.* 32, 155–164. doi:10.1007/s00269-005-0449-8

Di Benedetto, F., Bernardini, G. P., Cipriani, C., Emiliani, C., Gatteschi, D., and Romanelli, M. (2005). The Distribution of Cu(II) and the Magnetic Properties of the Synthetic Analogue of Tetrahedrite: Cu12Sb4S13. *Phys. Chem. Miner.* 32, 155–164. doi:10.1007/s00269-005-0449-8

Dong, Y., Khabibullin, A. R., Wei, K., Salvador, J. R., Nolas, G. S., and Woods, L. M. (2015). Bournonite PbCuSbS3: Stereochemically Active Lone-Pair Electrons that Induce Low Thermal Conductivity. *ChemPhysChem* 16, 3264–3270. doi:10.1002/cphc.201500476

Dong, Z., Jiang, T., Xu, B., Zhong, H., Zhang, B., Liu, G., et al. (2021). Density Functional Theory Study on Electronic Structure of Tetrahedrite and Effect of Natural Impurities on its Flotation Property. *Miner. Eng.* 169, 106980. doi:10.1016/j.mineng.2021.106980

Dresselhaus, M. S., Chen, G., Tang, M. Y., Yang, R. G., Lee, H., Wang, D. Z., et al. (2007). New Directions for Low-Dimensional Thermoelectric Materials. *Adv. Mat.* 19, 1043–1053. doi:10.1002/adma.200600527

Du, B., Chen, K., Yan, H., and Reece, M. J. (2016). Efficacy of Lone-Pair Electrons to Engender Ultralow Thermal Conductivity. *Scr. Mater.* 111, 49–53. doi:10.1016/j.scriptamat.2015.05.031

Du, B., Zhang, R., Chen, K., Mahajan, A., and Reece, M. J. (2017). The Impact of Lone-Pair Electrons on the Lattice Thermal Conductivity of the Thermoelectric Compound CuSbS2. *J. Mat. Chem. A* 5, 3249–3259. doi:10.1039/c6ta10420g

Fan, X., Case, E. D., Lu, X., and Morelli, D. T. (2013). Room Temperature Mechanical Properties of Natural-Mineral-Based Thermoelectrics. *J. Mater Sci.* 48, 7540–7550. doi:10.1007/s10853-013-7569-1

Geballe, T. H., and Hull, G. W. (1955). Seebeck Effect in Silicon. *Phys. Rev.* 98, 940–947. doi:10.1103/physrev.98.940

Ghassemi, N., Lu, X., Tian, Y., Conant, E., Yan, Y., Zhou, X., et al. (2018). Structure Change and Rattling Dynamics in Cu12Sb4S13 Tetrahedrite: an NMR Study. *ACS Appl. Mat. Interfaces* 10, 36010–36017. doi:10.1021/acsami.8b13646

Goldsmid, H. J. (1960). *Applications of Thermoelectricity*. London: Methuen.

Goldsmid, H. J., and Douglas, R. W. (1954). The Use of Semiconductors in Thermoelectric Refrigeration. *Br. J. Appl. Phys.* 5, 386–390. doi:10.1088/0508-3443/5/11/303

Gonçalves, A. P., Lopes, E. B., Villeroy, B., Monnier, J., Godart, C., and Lenoir, B. (2016). Effect of Ni, Bi and Se on the Tetrahedrite Formation. *RSC Adv.* 6, 102359–102367. doi:10.1039/c6ra21482g

Gondim, M. F., Maestrelli, S. C., Ramos, E. C. T., Rodrigues, J. A. J., and Ramos, A. S. (2015). Synthesis of TaAlO4 Compound and Al2O3-TaAlO4 Composite Ceramic by Mechanical Alloying and Their Sintering. *Ceram. Int.* 41, 2260–2265. doi:10.1016/j.ceramint.2014.10.029

Goryunova, N. A. (1965). *The Chemistry of Diamond-Like Semiconductors*. Cambridge, MA: MIT Press.

Guillon, O., Gonzalez-Julian, J., Dargatz, B., Kessel, T., Schierning, G., Räthel, J., et al. (2014). Field-Assisted Sintering Technology/Spark Plasma Sintering: Mechanisms, Materials, and Technology Developments. *Adv. Eng. Mat.* 16, 830–849. doi:10.1002/adem.201300409

Guler, A., Boyraz, C., Shulgin, D. A., Mozzhukhin, G. V., and Rameev, B. Z. (2016). in 9th Int. Kharkiv Symposium on Physics and Engineering of Microwaves, Millimeter and Submillimeter Waves, 2016, 1.

Harish, S., Sivaprahasam, D., Battabyal, M., and Gopalan, R. (2016). Phase Stability and Thermoelectric Properties of Cu10.5Zn1.5Sb4S13 Tetrahedrite. *J. Alloys Compd.* 667, 323–328. doi:10.1016/j.jallcom.2016.01.094

Heo, J., Laurita, G., Muir, S., Subramanian, M. A., and Keszler, D. A. (2014). Enhanced Thermoelectric Performance of Synthetic Tetrahedrites. *Chem. Mat.* 26, 2047–2051. doi:10.1021/cm404026k

Huang, L. L., Wang, Y. S., Zhu, C., Xu, R., Li, J. M., Zhang, J. H., et al. (2018). Preparation and Enhanced Thermoelectric Performance of Pb-Doped Tetrahedrite Cu12-xPbxSb4S13. *J. Alloys Compd.* 769, 478–483. doi:10.1016/j.jallcom.2018.07.335

Hulbert, D. M., Anders, A., Dudina, D. V., Andersson, J., Jiang, D., Unuvar, C., et al. (2008). The Absence of Plasma in "spark Plasma Sintering". *J. Appl. Phys.* 104, 033305. doi:10.1063/1.2963701

Ioffe, A. F. (1957). *Semiconductor Thermoelements and Thermoelectric Cooling*. London: Infosearch, Ltd.

James, D. J., Lu, X., Morelli, D. T., and Brock, S. L. (2015). Solvothermal Synthesis of Tetrahedrite: Speeding up the Process of Thermoelectric Material Generation. *ACS Appl. Mat. Interfaces* 7, 23623–23632. doi:10.1021/acsami.5b07141

Jeanloz, R., and Johnson, M. L. (1984). A Note on the Bonding, Optical Spectrum and Composition of Tetrahedrite. *Phys. Chem. Miner.* 11, 52–54. doi:10.1007/bf00309375

John, B., Genifer Silvena, G., and Leo Rajesh, A. (2018). Influence of Reaction Time on the Structural, Optical and Electrical Performance of Copper Antimony Sulfide Nanoparticles Using Solvothermal Method. *Phys. B Condens. Matter* 537, 243–250. doi:10.1016/j.physb.2018.02.030

Johnson, M. L., and Jeanloz, R. (1983). A Brillouin-Zone Model for Compositional Variation in Tetrahedrite. *Am. Min.* 68, 220–226.

Johnson, N. E., Craig, J. R., and Rimstidt, J. D. (1986). Compositional Trends in Tetrahedrite. *Can. Min.* 24, 385.

Johnson, N. E., Craig, J. R., and Rimstidt, J. D. (1988). Crystal Chemistry of Tetrahedrite. *Am. Min.* 73, 389.

Julian, C. L. (1963). Theory of Heat Conduction in Rare-Gas Crystals. *Phys. Rev.* 137, A128.

Karthiselva, N. S., Murty, B. S., and Bakshi, S. R. (2015). Low Temperature Synthesis of Dense TiB2 Compacts by Reaction Spark Plasma Sintering. *Int. J. Refract. Metals Hard Mater.* 48, 201–210. doi:10.1016/j.ijrmhm.2014.09.015

Kim, S.-Y., Kwak, S.-G., Pi, J.-H., Lee, G.-E., and Kim, I.-H. (2019). Preparation of Tetrahedrite Cu12Sb4S13 by Mechanical Alloying and Hot Pressing. *J. Elec Materi* 48, 1857–1863. doi:10.1007/s11664-018-6549-2

Kim, S.-Y., Lee, G.-E., and Kim, I.-H. (2019). Thermoelectric Properties of Mechanically-Alloyed and Hot-Pressed Cu12−xCoxSb4S13 Tetrahedrites. *J. Korean Phys. Soc.* 74, 967–971. doi:10.3938/jkps.74.967

Kim, S.-Y., Pi, J.-H., Lee, G.-E., and Kim, I.-H. (2020). Synthesis of Fe-Doped Tetrahedrites Cu12-xFexSb4S13 and Characterization of Their Thermoelectric Properties. *Korean J. Met. Mat.* 58, 340–347. doi:10.3365/kjmm.2020.58.5.340

Kitagawa, S., Sekiya, T., Araki, S., Kobayashi, T., Ishida, K., Kambe, T., et al. (2015). Suppression of Nonmagnetic Insulating State by Application of Pressure in Mineral Tetrahedrite Cu12Sb4S13. *J. Phys. Soc. Jpn.* 84, 1. doi:10.7566/jpsj.84.093701

Klemens, P. G. (1960). Thermal Resistance Due to Point Defects at High Temperatures. *Phys. Rev.* 119, 507–509. doi:10.1103/physrev.119.507

Kosaka, Y., Suekuni, K., Hashikuni, K., Bouyrie, Y., Ohta, M., and Takabatake, T. (2017). Effects of Ge and Sn Substitution on the Metal-Semiconductor Transition and Thermoelectric Properties of Cu12Sb4S13 Tetrahedrite. *Phys. Chem. Chem. Phys.* 19, 8874–8879. doi:10.1039/c7cp00351j

Kwak, S.-G., Lee, G.-E., and Kim, I.-H. (2021). Electronic Transport and Thermoelectric Properties of Te-Doped Tetrahedrites Cu12Sb4-yTeyS13. *Korean J. Met. Mat.* 59, 560–566. doi:10.3365/kjmm.2021.59.8.560

Kwak, S.-G., Pi, J.-H., Lee, G.-E., and Kim, I.-H. (2020). Solid-State Synthesis and Thermoelectric Properties of Tetrahedrites Cu12Sb4-yBiyS13. *Korean J. Met. Mat.* 58, 272–277. doi:10.3365/kjmm.2020.58.4.272

Lai, W., Wang, Y., Morelli, D. T., and Lu, X. (2015). From Bonding Asymmetry to Anharmonic Rattling in Cu12Sb4S13Tetrahedrites: When Lone-Pair Electrons Are Not So Lonely. *Adv. Funct. Mat.* 25, 3648–3657. doi:10.1002/adfm.201500766

Lara-Curzio, E., May, A. F., Delaire, O., Mcguire, M. A., Lu, X., Liu, C.-Y., et al. (2014). Low-temperature Heat Capacity and Localized Vibrational Modes in Natural and Synthetic Tetrahedrites. *J. Appl. Phys.* 115, 193515. doi:10.1063/1.4878676

Lawson, A. W. (1957). On the High Temperature Heat Conductivity of Insulators. *J. Phys. Chem. Solids* 3, 155–156. doi:10.1016/0022-3697(57)90064-1

Leibfried, G., and Schlömann, E. (1954). Nachr.Akad.Wiss.Gottingen Math.Phys.Kl.II. *Nachr. Akad. Wiss. Göttingen II* a (4), 71.

Levinsky, P., Candolfi, C., Dauscher, A., Lenoir, B., and Hejtmánek, J. (2019). Thermoelectric Properties of Magnesium-Doped Tetrahedrite Cu12−xMgxSb4S13. *J. Elec Materi* 48, 1926–1931. doi:10.1007/s11664-019-07032-w

Li, C. W., Hong, J., May, A. F., Bansal, D., Chi, S., Hong, T., et al. (2015). Orbitally Driven Giant Phonon Anharmonicity in SnSe. *Nat. Phys.* 11, 1063–1069. doi:10.1038/nphys3492

Li, J., Weller, D. P., Morelli, D. T., and Lai, W. (2018). Density-functional Theory Based Molecular Dynamics Simulation of Tetrahedrite Thermoelectrics: Effect of Cell Size and Basis Sets. *Comput. Mater. Sci.* 144, 315–321. doi:10.1016/j.commatsci.2017.12.047

Li, J., Zhu, M., Abernathy, D. L., Ke, X., Morelli, D. T., and Lai, W. (2016). First-principles Studies of Atomic Dynamics in Tetrahedrite Thermoelectrics. *Apl. Mater.* 4, 104811. doi:10.1063/1.4959961

Liu, R., Xi, L., Liu, H., Shi, X., Zhang, W., and Chen, L. (2012). Ternary Compound CuInTe2: a Promising Thermoelectric Material with Diamond-like Structure. *Chem. Commun.* 48, 3818. doi:10.1039/c2cc30318c

Locci, A. M., Licheri, R., Orrù, R., and Cao, G. (2009). Reactive Spark Plasma Sintering of Rhenium Diboride. *Ceram. Int.* 35, 397–400. doi:10.1016/j.ceramint.2007.11.012

Lu, X., and Morelli, D. (2014). The Effect of Te Substitution for Sb on Thermoelectric Properties of Tetrahedrite. *J. Elec Materi* 43, 1983–1987. doi:10.1007/s11664-013-2931-2

Lu, X., and Morelli, D. T. (2013). Natural Mineral Tetrahedrite as a Direct Source of Thermoelectric Materials. *Phys. Chem. Chem. Phys.* 15, 5762. doi:10.1039/c3cp50920f

Lu, X., and Morelli, D. T. (2013). Rapid Synthesis of High-Performance Thermoelectric Materials Directly from Natural Mineral Tetrahedrite. *MRS Commun.* 3, 129–133. doi:10.1557/mrc.2013.26

Lu, X., Morelli, D. T., Wang, Y., Lai, W., Xia, Y., and Ozolins, V. (2016). Phase Stability, Crystal Structure, and Thermoelectric Properties of Cu12Sb4S13-xSex Solid Solutions. *Chem. Mat.* 28, 1781–1786. doi:10.1021/acs.chemmater.5b04796

Lu, X., Morelli, D. T., Xia, Y., and Ozolins, V. (2015). Increasing the Thermoelectric Figure of Merit of Tetrahedrites by Co-doping with Nickel and Zinc. *Chem. Mat.* 27, 408–413. doi:10.1021/cm502570b

Lu, X., Morelli, D. T., Xia, Y., Zhou, F., Ozolins, V., Chi, H., et al. (2013). High Performance Thermoelectricity in Earth-Abundant Compounds Based on Natural Mineral Tetrahedrites. *Adv. Energy Mat.* 3, 342–348. doi:10.1002/aenm.201200650

Makovicky, E., Forcher, K., Lottermoser, W., and Amthauer, G. (1990). The Role of Fe2+ and Fe3+ in Synthetic Fe-Substituted Tetrahedrite. *Mineralogy Petrology* 43, 73–81. doi:10.1007/bf01164223

Makovicky, E., and Moller, S. K. (1994). Partition Coefficients for Ni, Cu, Pd, Pt, Rh and Ir between Monosulphide Solid Solution and Sulphide Liquid and the Implications for the Formation of Compositionally Zoned Ni-Cu Sulphide Bodies by Fractional Crystallization of Sulphide Liquid. *Neues Jahrb. Min. Abh.* 167, 89.

Makovicky, E., and Skinner, B. J. (1979). Studies of the Sulfosalts of Copper; VI, Low-Temperature Exsolution in Synthetic Tetrahedrite Solid Solution, Cu (Sub 12+x) Sb (Sub 4+y) S 13. *Can. Min.* 17, 619.

May, A. F., Delaire, O., Niedziela, J. L., Lara-Curzio, E., Susner, M. A., Abernathy, D. L., et al. (2016). Structural Phase Transition and Phonon Instability in Cu12Sb4S13. *Phys. Rev. B* 93, 064104. doi:10.1103/physrevb.93.064104

Mishra, T. P., Koyano, M., and Oshima, Y. (2017). Detection of Large Thermal Vibration for Cu Atoms in Tetrahedrite by High-Angle Annular Dark-Field Imaging. *Appl. Phys. Express* 10, 045601. doi:10.7567/apex.10.045601

Moller, S. K., and Makovicky, E. (1999). The System Pd-Fe-Ni-S at 900 and 725. *Neuses Jahrb. Fur Monatsh.* 9, 385.

Morelli, D. T. (2017). in *Material Aspects of Thermoelectricity*. Editor C. Uher (Boca Raton, FL: CRC Press), 473.

Mozgova, N., Mikučionis, V., Valiukenas, V. I., Tsepin, A., and Orliukas, A. (1987). Some Electrical Properties of Fahlore Cu10(Zn,Fe)2(As,Sb)4S13. *Phys. Chem. Miner.* 15, 171–172. doi:10.1007/bf00308780

Nasonova, D. I., Presniakov, I. A., Sobolev, A. V., Verchenko, V. Y., Tsirlin, A. A., Wei, Z., et al. (2016). Role of Iron in Synthetic Tetrahedrites Revisited. *J. Solid State Chem.* 242, 62–69. doi:10.1016/j.jssc.2016.03.009

Nasonova, D. I., Verchenko, V. Y., Tsirlin, A. A., and Shevelkov, A. V. (2016). Low-Temperature Structure and Thermoelectric Properties of Pristine Synthetic Tetrahedrite Cu12Sb4S13. *Chem. Mat.* 28, 6621–6627. doi:10.1021/acs.chemmater.6b02720

Nielsen, M. D., Ozolins, V., and Heremans, J. P. (2013). Lone Pair Electrons Minimize Lattice Thermal Conductivity. *Energy Environ. Sci.* 6, 570–578. doi:10.1039/c2ee23391f

Nolas, G. S. (2002). *Chemistry, Physics, and Materials Science of Thermoelectric Materials*. Editors M. G. Kanatzidis, S. D. Mahanti, and T. P. Hogan (New York: Springer), 107.

Orrù, R., and Cao, G. (2013). Comparison of Reactive and Non-reactive Spark Plasma Sintering Routes for the Fabrication of Monolithic and Composite Ultra High Temperature Ceramics (UHTC) Materials. *Materials* 6, 1566–1583. doi:10.3390/ma6051566

Parashchuk, T., Wiendlocha, B., Cherniushok, O., Knura, R., and Wojciechowski, K. T. (2021). High Thermoelectric Performance of P-type PbTe Enabled by the Synergy of Resonance Scattering and Lattice Softening. *ACS Appl. Mat. Interfaces* 13, 49027–49042. doi:10.1021/acsami.1c14236

Pattrick, R. A. D., and Hall, A. J. (1983). Silver Substitution into Synthetic Zinc, Cadmium, and Iron Tetrahedrites. *Mineral. Mag.* 47, 441–451. doi:10.1180/minmag.1983.047.345.05

Pattrick, R. A. D., van der Laan, G., Vaughan, D. J., and Henderson, C. M. B. (1993). Oxidation State and Electronic Configuration Determination of Copper in Tetrahedrite Group Minerals by L-Edge X-Ray Absorption Spectroscopy. *Phys. Chem. Miner.* 20, 395–401. doi:10.1007/bf00203108

Pfitzner, A., Evain, M., and Petricek, V. (1997). Cu12Sb4S13: A Temperature-dependent Structure Investigation. *Acta Crystallogr. Sect. B* 53, 337–345. doi:10.1107/s0108768196014024

Pi, J.-H., Kwak, S.-G., Kim, S.-Y., Lee, G.-E., and Kim, I.-H. (2019). Thermal Stability and Mechanical Properties of Thermoelectric Tetrahedrite Cu12Sb4S13. *J. Elec Materi* 48, 1991–1997. doi:10.1007/s11664-018-06883-z

Plirdpring, T., Kurosaki, K., Kosuga, A., Day, T., Firdosy, S., Ravi, V., et al. (2012). Chalcopyrite CuGaTe2: A High-Efficiency Bulk Thermoelectric Material. *Adv. Mat.* 24, 3622–3626. doi:10.1002/adma.201200732

Prem Kumar, D. S., Chetty, R., Femi, O. E., Chattopadhyay, K., Malar, P., and Mallik, R. C. (2016). Thermoelectric Properties of Bi Doped Tetrahedrite. *J. Elec Materi* 46, 2616–2622. doi:10.1007/s11664-016-4826-5

Prem Kumar, D. S., Chetty, R., Rogl, P., Rogl, G., Bauer, E., Malar, P., et al. (2016). Thermoelectric Properties of Cd Doped Tetrahedrite: Cu12−xCdxSb4S13. *Intermetallics* 78, 21–29. doi:10.1016/j.intermet.2016.08.003

Prem Kumar, D. S., Ren, M., Osipowicz, T., Mallik, R. C., and Malar, P. (2018). Tetrahedrite (Cu12Sb4S13) Thin Films for Photovoltaic and Thermoelectric Applications. *Sol. Energy* 174, 422–430. doi:10.1016/j.solener.2018.08.080

Qiu, P., Zhang, T., Qiu, Y., Shi, X., and Chen, L. (2014). Sulfide Bornite Thermoelectric Material: a Natural Mineral with Ultralow Thermal Conductivity. *Energy Environ. Sci.* 7, 400. doi:10.1039/c4ee02428a

Ramasamy, K., Sims, H., Butler, W. H., and Gupta, A. (2014). Selective Nanocrystal Synthesis and Calculated Electronic Structure of All Four Phases of Copper-Antimony-Sulfide. *Chem. Mat.* 26, 2891–2899. doi:10.1021/cm5005642

Rath, T., Maclachlan, A. J., Brown, M. D., and Haque, S. A. (2015). Structural, Optical and Charge Generation Properties of Chalcostibite and Tetrahedrite Copper Antimony Sulfide Thin Films Prepared from Metal Xanthates. *J. Mat. Chem. AJournal Mater. Chem. A* 3, 24155–24162. doi:10.1039/c5ta05777a

Sahin, F. C., Kanbur, H. E., and Apak, B. (2012). Preparation of AlON Ceramics via Reactive Spark Plasma Sintering. *J. Eur. Ceram. Soc.* 32, 925–929. doi:10.1016/j.jeurceramsoc.2011.10.043

Seal, R. R., Essene, E. J., and Kelly, W. C. (1990). Tetrahedrite and Tennantite; Evaluation of Thermodynamic Data and Phase Equilibria. *Can. Min.* 28, 725.

Skoug, E. J., Cain, J. D., and Morelli, D. T. (2011). High Thermoelectric Figure of Merit in the Cu3SbSe4-Cu3SbS4solid Solution. *Appl. Phys. Lett.* 98, 261911. doi:10.1063/1.3605246

Skoug, E. J., Cain, J. D., and Morelli, D. T. (2010). Thermoelectric Properties of the Cu2SnSe3-Cu2GeSe3 Solid Solution. *J. Alloys Compd.* 506, 18–21. doi:10.1016/j.jallcom.2010.06.182

Skoug, E. J., and Morelli, D. T. (2011). Role of Lone-Pair Electrons in Producing Minimum Thermal Conductivity in Nitrogen-Group Chalcogenide Compounds. *Phys. Rev. Lett.* 107, 235901. doi:10.1103/physrevlett.107.235901

Slack, G. A. (1995). in *CRC Handbook of Thermoelectrics*. Editor D. M. Rowe (Boca Raton: CRC Press), 407.

Stavila, V., Robinson, D. B., Hekmaty, M. A., Nishimoto, R., Medlin, D. L., Zhu, S., et al. (2013). Wet-Chemical Synthesis and Consolidation of Stoichiometric Bismuth Telluride Nanoparticles for Improving the Thermoelectric Figure-Of-Merit. *ACS Appl. Mat. Interfaces* 5, 6678–6686. doi:10.1021/am401444w

Suehiro, S., Horita, K., Yuasa, M., Tanaka, T., Fujita, K., Ishiwata, Y., et al. (2015). Synthesis of Copper-Antimony-Sulfide Nanocrystals for Solution-Processed Solar Cells. *Inorg. Chem.* 54, 7840–7845. doi:10.1021/acs.inorgchem.5b00858

Suekuni, K., Lee, C. H., Tanaka, H. I., Nishibori, E., Nakamura, A., Kasai, H., et al. (2018). Retreat from Stress: Rattling in a Planar Coordination. *Adv. Mat.* 30, 1706230. doi:10.1002/adma.201706230

Suekuni, K., Tomizawa, Y., Ozaki, T., and Koyano, M. (2014). Systematic Study of Electronic and Magnetic Properties for Cu12-xTMxSb4S13 (TM = Mn, Fe, Co, Ni, and Zn) Tetrahedrite. *J. Appl. Phys.* 115, 143702. doi:10.1063/1.4871265

Suekuni, K., Tsuruta, K., Ariga, T., and Koyano, M. (2012). Thermoelectric Properties of Mineral Tetrahedrites Cu$_{10}$Tr$_{2}$Sb$_{4}$S$_{13}$ with Low Thermal Conductivity. *Appl. Phys. Express* 5, 051201. doi:10.1143/apex.5.051201

Suekuni, K., Tsuruta, K., Kunii, M., Nishiate, H., Nishibori, E., Maki, S., et al. (2013). High-performance Thermoelectric Mineral

Cu12−xNixSb4S13tetrahedrite. *J. Appl. Phys.* 113, 043712. doi:10.1063/1.4789389

Sun, F.-H., Wu, C.-F., Li, Z., Pan, Y., Asfandiyar, A., Dong, J., et al. (2017). Powder Metallurgically Synthesized Cu12Sb4S13tetrahedrites: Phase Transition and High Thermoelectricity. *RSC Adv.* 7, 18909–18916. doi:10.1039/c7ra02564e

Sun, S.-K., Zhang, G.-J., Wu, W.-W., Liu, J.-X., Suzuki, T., and Sakka, Y. (2013). Reactive Spark Plasma Sintering of ZrC and HfC Ceramics with Fine Microstructures. *Scr. Mater.* 69, 139–142. doi:10.1016/j.scriptamat.2013.02.017

Suryanarayana, C., Ivanov, E., and Boldyrev, V. V. (2001). The Science and Technology of Mechanical Alloying. *Mater. Sci. Eng. A* 304-306, 151–158. doi:10.1016/s0921-5093(00)01465-9

Suzuki, T., Goto, H., Ishii, I., Noguchi, Y., Kamikawa, S., Suekuni, K., et al. (2015). Elastic Softening in the Tetrahedrite Cu12Sb4S13. *Phys. Procedia* 75, 443–446. doi:10.1016/j.phpro.2015.12.054

Tablero, C. (2014). Electronic and Optical Property Analysis of the Cu-Sb-S Tetrahedrites for High-Efficiency Absorption Devices. *J. Phys. Chem. C* 118, 15122–15127. doi:10.1021/jp502045w

Tanaka, H. I., Suekuni, K., Umeo, K., Nagasaki, T., Sato, H., Kutluk, G., et al. (2016). Metal-Semiconductor Transition Concomitant with a Structural Transformation in Tetrahedrite Cu12Sb4S13. *J. Phys. Soc. Jpn.* 85, 014703. doi:10.7566/jpsj.85.014703

Tatsuka, K., and Morimoto, N. (1973). Composition Variation and Polymorphism of Tetrahedrite in the Cu-Sb-S System below 400°C. *Am. Min.* 58, 425.

Tatsuka, K., and Morimoto, N. (1977). Tetrahedrite Stability Relations in the Cu-Sb-S System. *Econ. Geol.* 72, 258–270. doi:10.2113/gsecongeo.72.2.258

Tippireddy, S., Chetty, R., Naik, M. H., Jain, M., Chattopadhyay, K., and Mallik, R. C. (2018). Electronic and Thermoelectric Properties of Transition Metal Substituted Tetrahedrites. *J. Phys. Chem. C* 122, 8735–8749. doi:10.1021/acs.jpcc.7b12214

Tippireddy, S., Chetty, R., Raut, K. K., Naik, M. H., Mukharjee, P. K., Jain, M., et al. (2018). Electronic and Thermoelectric Properties of Zn and Se Double Substituted Tetrahedrite. *Phys. Chem. Chem. Phys.* 20, 28667–28677. doi:10.1039/c8cp05479g

Tippireddy, S., Ghosh, S., Biswas, R., Dasgupta, T., Rogl, G., Rogl, P., et al. (2020). Thermoelectric Properties of Al Substituted Tetrahedrite. *J. Appl. Phys.* 127, 035105. doi:10.1063/1.5128409

Tippireddy, S., Prem Kumar, D. S., Karati, A., Ramakrishnan, A., Sarkar, S., Peter, S. C., et al. (2019). Effect of Sn Substitution on the Thermoelectric Properties of Synthetic Tetrahedrite. *ACS Appl. Mat. Interfaces* 11, 21686–21696. doi:10.1021/acsami.9b02956

US Department of Energy, Lawrence Livermore National Laboratory (2016). *Estimated Energy Flow Chart*. Availableat: https://flowcharts.llnl.gov/.

van Embden, J., Latham, K., Duffy, N. W., and Tachibana, Y. (2013). Near-Infrared Absorbing Cu12Sb4S13 and Cu3SbS4 Nanocrystals: Synthesis, Characterization, and Photoelectrochemistry. *J. Am. Chem. Soc.* 135, 11562–11571. doi:10.1021/ja402702x

Vaqueiro, P., Al Orabi, R. A. R., Luu, S. D. N., Guélou, G., Powell, A. V., Smith, R. I., et al. (2015). The Role of Copper in the Thermal Conductivity of Thermoelectric Oxychalcogenides: Do Lone Pairs Matter? *Phys. Chem. Chem. Phys.* 17, 31735–31740. doi:10.1039/c5cp06192j

Vaqueiro, P., Guélou, G., Kaltzoglou, A., Smith, R. I., Barbier, T., Guilmeau, E., et al. (2017). The Influence of Mobile Copper Ions on the Glass-like Thermal Conductivity of Copper-Rich Tetrahedrites. *Chem. Mat.* 29, 4080–4090. doi:10.1021/acs.chemmater.7b00891

Wang, J., Gu, M., Bao, Y., Li, X., and Chen, L. (2016). Quick Fabrication and Thermoelectric Properties of Cu12Sb4S13 Tetrahedrite. *J. Elec Materi* 45, 2274–2277. doi:10.1007/s11664-015-4301-8

Wang, L., Jiang, W., Chen, L., and Bai, S. (2004). Rapid Reactive Synthesis and Sintering of Submicron TiC/SiC Composites through Spark Plasma Sintering. *J. Am. Ceram. Soc.* 87, 1157–1160. doi:10.1111/j.1551-2916.2004.01157.x

Weller, D. P., Kunkel, G. E., Ochs, A. M., Morelli, D. T., and Anderson, M. E. (2018). Observation of N-type Behavior in Fe-Doped Tetrahedrite at Low Temperature. *Mater. Today Phys.* 7, 1–6. doi:10.1016/j.mtphys.2018.10.003

Weller, D. P., and Morelli, D. T. (2017). Rapid Synthesis of Zinc and Nickel Co-doped Tetrahedrite Thermoelectrics by Reactive Spark Plasma Sintering and Mechanical Alloying. *J. Alloys Compd.* 710, 794–799. doi:10.1016/j.jallcom.2017.03.272

Weller, D. P., Stevens, D. L., Kunkel, G. E., Ochs, A. M., Holder, C. F., Morelli, D. T., et al. (2017). Thermoelectric Performance of Tetrahedrite Synthesized by a Modified Polyol Process. *Chem. Mat.* 29, 1656–1664. doi:10.1021/acs.chemmater.6b04950

Wu, W.-W., Zhang, G.-J., Kan, Y.-M., Wang, P.-L., Vanmeensel, K., Vleugels, J., et al. (2007). Synthesis and Microstructural Features of ZrB2-SiC-Based Composites by Reactive Spark Plasma Sintering and Reactive Hot Pressing. *Scr. Mater.* 57, 317–320. doi:10.1016/j.scriptamat.2007.04.025

Wu, Y., Qiao, X., Fan, X., Zhang, X., Cui, S., and Wan, J. (2015). Facile Synthesis of Monodisperse Cu3SbSe4 Nanoparticles and Thermoelectric Performance of Cu3SbSe4 Nanoparticle-Based Materials. *J. Nanoparticle Res.* 17, 1. doi:10.1007/s11051-015-3094-2

Wuensch, B. J. (1964). The Crystal Structure of Tetrahedrite, Cu12Sb4S13. *Z. für Kristallogr.* 119, 437–453. doi:10.1524/zkri.1964.119.5-6.437

Yan, Y., Wu, H., Wang, G., Lu, X., and Zhou, X. (2018). High Thermoelectric Performance Balanced by Electrical and Thermal Transport in Tetrahedrites Cu12+Sb4S12Se. *Energy Storage Mater.* 13, 127–133. doi:10.1016/j.ensm.2018.01.006

Zazakowny, K., Kosonowski, A., Lis, A., Cherniushok, O., Parashchuk, T., Tobola, J., et al. (2022). Phase Analysis and Thermoelectric Properties of Cu-Rich Tetrahedrite Prepared by Solvothermal Synthesis. *Materials* 15, 849. doi:10.3390/ma15030849

Zhang, Y., Ozoliņš, V., Morelli, D., and Wolverton, C. (2014). Prediction of New Stable Compounds and Promising Thermoelectrics in the Cu-Sb-Se System. *Chem. Mat.* 26, 3427–3435. doi:10.1021/cm5006828

Zhao, Y., Wang, L. J., Zhang, G. J., Jiang, W., and Chen, L. D. (2007). Preparation and Microstructure of a ZrB2–SiC Composite Fabricated by the Spark Plasma Sintering–Reactive Synthesis (SPS–RS) Method. *J. Am. Ceram. Soc.* 90, 4040. doi:10.1111/j.1551-2916.2007.02050.x

Zhou, F., Nielson, W., Xia, Y., and Ozoliņš, V. (2014). Lattice Anharmonicity and Thermal Conductivity from Compressive Sensing of First-Principles Calculations. *Phys. Rev. Lett.* 113, 185501. doi:10.1103/physrevlett.113.185501

Zhu, C., Chen, Q., Ming, H., Qin, X., Yang, Y., Zhang, J., et al. (2021). Improved Thermoelectric Performance of Cu12Sb4S13 through Gd-Substitution Induced Enhancement of Electronic Density of States and Phonon Scattering. *ACS Appl. Mat. Interfaces* 13, 25092–25101. doi:10.1021/acsami.1c03493

Conflict of Interest: The authors declare that the research was conducted in the absence of any commercial or financial relationships that could be construed as a potential conflict of interest.

Publisher's Note: All claims expressed in this article are solely those of the authors and do not necessarily represent those of their affiliated organizations, or those of the publisher, the editors and the reviewers. Any product that may be evaluated in this article, or claim that may be made by its manufacturer, is not guaranteed or endorsed by the publisher.